Supporting Information

Structure and Electrocatalytic Performance of Co-crystallized Ternary Molybdenum Oxo-sulfide Clusters for Efficient Water Splitting

Biswajit Mondal[1#], Arijit Jana[1#], Jayoti Roy[1#], Astrid Campos Mata[2], Akhil S Nair[3], Ananthu Mahendranath[1], Soumyabrata Roy[2], Biswarup Pathak[4]*, Pulickel M. Ajayan[2]* and Thalappil Pradeep[1,5]*

[1]DST Unit of Nanoscience (DST UNS) & Thematic Unit of Excellence (TUE), Department of Chemistry, Indian Institute of Technology Madras, Chennai 600036, India

[2]Department of Materials Science and NanoEngineering, Rice University, TX 77005, USA

[3]Department of Chemistry, Indian Institute of Technology Indore, Indore 453552, India. The NOMAD Laboratory at the FHI of the Max-Planck Gesellschaft and IRIS-Adlershof of the Humboldt-Universität zu Berlin, Germany.

[4]Department of Chemistry, Indian Institute of Technology Indore, Indore 453552, India

[5]International Centre for Clean Water, 2nd Floor, B-Block, IIT Madras Research Park, Kanagam Road, Taramani, Chennai 600113, India

Table of content

Experimental Section

Chemicals used

Sodium molybdate (Na_2MoO_4) was purchased from Merck. Sodium dithionite ($Na_2S_2O_4$) was bought from Merck. Sulphur powder was purchased from CDH. Phenylphosphonic acid was received from Spectrochem. 50% ammonium sulfide was brought from Sigma Aldrich. Hydrochloric acid was purchased from Merck. DI water was used for the synthesis. HPLC-grade solvents such as methanol were purchased from Rankem chemicals. All the chemicals are commercially available and used as such without any purification.

Synthesis of Mo_{12} clusters

In a typical synthesis, 0.86 g of Na_2MoO_4 was dissolved in 25 mL of DI water (step – 1). The pH of the solution was adjusted to ~3 by adding HCl (step – 2). Then, 0.4 g of S dissolved in 2 mL of 50% ammonium sulfide solution was added to aqueous solution of Na_2MoO_4 (step – 3). Upon addition of S, the color of the solution became dark brown. 0.133 g of $Na_2S_2O_4$ and 0.158 g of phenylphosphonic acid were added to the above reaction mixture and the reaction was continued overnight (step – 4, 5). Finally, it was centrifuged at 5000 rpm for 5 min to collect the precipitate. The cluster was extracted in methanol for further characterization and crystallization.

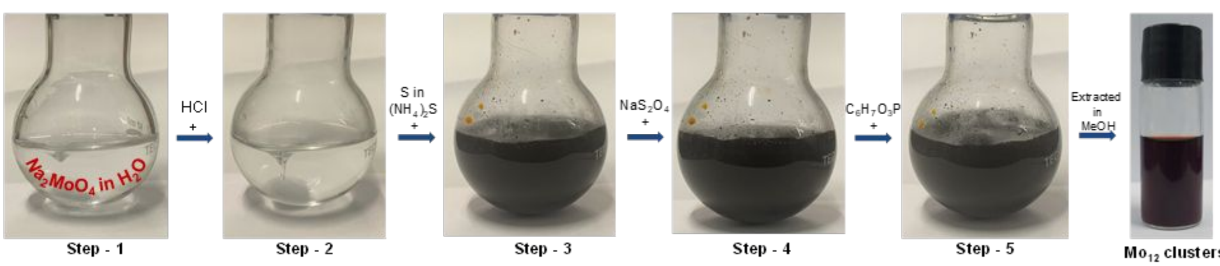

Schematic S1. Photographs of the reaction bottle showed the visual color changes during the synthesis of the Mo_{12} clusters.

Electrochemical studies

Electrochemical measurements for hydrogen evolution (HER) and oxygen evolution (OER) reactions were studied in a conventional three-electrode cell using an AUTOLAB electrochemical workstation. A graphite rod, a saturated calomel electrode (SCE), and the catalyst coated on glassy carbon (GC) electrode were used as the counter, reference, and working electrodes, respectively for HER. A mercury/mercuric oxide (Hg/HgO) electrode was used as reference electrode for OER studies. All measured potentials were converted to the reversible hydrogen electrode (RHE) values. The GC electrode (0.071 cm^2) was coated by catalyst ink (5 µL of 4 mg of the cluster, 1 mg Vulcan C, 10µL of nafion 1%, 125 µL of H_2O, and 125 isopropyl alcohol). HER studies were carried out under acidic conditions (0.5 M H_2SO_4) and OER studies under basic conditions (1M KOH).

Linear sweep voltammetry (LSV) experiments were conducted between -0.45 V to 0.2 V and 0.8V to 2.2 V, for HER and OER respectively, at scan rate of 5 mV s^{-1}. To evaluate the stability of our catalyst, accelerated degradation tests (ADT) using cyclic voltammetry (CV) studies we conducted between -0.356 V to -0.106 V (HER) and 1.29 V to 2.04 V (OER) for up to 5000 cycles, at scan rate of 50 mV s^{-1}. Electrochemical impedance spectroscopy (EIS) was performed for both HER and OER at a frequency range from 100 kHz to 0.1 Hz, at potential values of -0.256 V for HER and 1.74 V for OER.

Instrumentations

UV-Vis absorption spectroscopy

UV-Vis absorption spectra were measured using Perkin Elmer Lambda 365 UV-Vis spectrophotometer in the wavelength range of 1100 nm to 200 nm using a bandpass filter of 1 nm. Purified cluster after extracting in MeOH was used for the measurements.

Mass spectrometry

All high-resolution electrospray ionization mass spectrometry (ESI MS) studies were performed using a Waters Synapt G2-Si high-definition mass spectrometer (HDMS). All MS measurements were acquired in the negative ion mode. The capillary voltage, cone voltage, and source offset were kept at 2.75 kV, 50-60 V, and 30-40 V, respectively, throughout the ESI MS measurements to obtain a well-resolved mass spectrum of Mo-S NC. The source and desolvation temperatures were maintained at 100 and 150 ℃, respectively. The desolvation gas flow was set at 500 l h^{-1} during the measurements. For the collision-induced dissociation (CID) study in the instrument, the mass-selected ions were passed through the trap, ion-mobility, and transfer cells before entering the time-of-flight mass analyzer. The CID was performed only in the trap cell, while the other collision cells were kept off. No extra voltages were applied in the IMS and transfer cells to avoid additional ions fragmentation. The collision energy (CE) in the trap varied between 0 and 200 CE (instrumental units) during CID MS study.

Transmission electron microscopy

Transmission electron micrographs were collected using JEOL 3010 at an operating voltage of 100 kV (to reduce beam-induced damage) with an ultrahigh-resolution (UHR) polepiece. This has a filament made up of LaB_6. The instrument works under a vacuum in the range 10^{-5} to 10^{-6} Pa. Gatan Orius SC200 CCD camera (2K x 2K) was used to collect the images. Before the imaging, a few single crystals were separated and ground with a mortar and pestle. Then, it was drop-cased on a carbon coated 300 mesh copper grid after suspending in MeOH.

Single crystal XRD

Single-crystal X-ray diffraction studies were performed at 296 K using Bruker D8 VENTURE instrument. The diffractometer is equipped with a Cu Kα X-ray source with the wavelength 1.54178 Å. A PHOTON 100 CMOS detector has been used to record the diffraction spots of different frames. A suitable crystal was mounted on a Kapton polymer loop with the help of paratone oil. The program APEX3-SAINT (Bruker, 2016) was used for integrating the frames. A multi-scan absorption correction was done using the program SADABS (Bruker, 2016). The structure was solved by SHELXT-2014 (Sheldrick, 2014) and refined by full-matrix least squares techniques using SHELXL-2018 (Sheldrick, 2018) computer program. Hydrogen atoms were fixed at calculated positions and refined as riding model with C-H = 0.93 Å and Uiso(H) = 1.2 Ueq©. Mercury 2020.2.0 and VESTA software have been used for the visualization of the structure and electron density modelling.

Theoretical calculations

A single cluster unit of the Mo_{12} structure is considered for the theoretical study. The periodic DFT calculations were done using Vienna Ab-Initio Simulation Package (VASP) by using Generalized gradient approximation of Perdew–Burke–Ernzerhof (PBE) functional.[1–3] Projector augmented wave (PAW) method is used for treating ion-electron interactions.[4,5] The ionic relaxations have been carried out using a conjugate gradient algorithm with convergence criteria of 10^{-4} eV for minimum energy and 0.05 eV $Å^{-1}$ for Hellmann-Feynman forces on atoms. Due to the large size of the unit cells of the compounds, the Brillouin zone was sampled at the Gamma point (1×1×1).

For the projected density of states (PDOS) calculation, a higher (2×2×2) K-mesh is used. For identifying the intercluster interactions, calculations of dimer and monomer clusters units are carried out with and without applying van der Waals correction using DFT-D3 method.

The molecular DFT calculations were done using Gaussian 09 D.01 program.[6] B3LYP functional with Pople's 6–31G* basis set was used for non-metal elements and LANL2DZ-ECP (effective core potential) was employed for Co atoms, respectively.[7, 8] The TD-DFT calculations considered 300 excited states.

Table S1. Crystal data and structure refinement

Identification code	NaMo12 cocrystal	
Empirical formula	Mo12 Na O54 P8 C48 H40	
Formula weight	2902.86	
Temperature	296(2) K	
Wavelength	1.54178 Å	
Crystal system	Monoclinic	
Space group	$P2_1/c$	
Unit cell dimensions	a = 18.1456(7) Å	α= 90°.
	B = 13.8107(5) Å	β= 108.052(3)°.
	C = 20.6756(9) Å	γ = 90°.
Volume	4926.3(3) $Å^3$	
Z	2	
Density (calculated)	2.070 Mgm^{-3}	
Absorption coefficient	14.612 mm^{-1}	
F(000)	2966	
Crystal size	0.150 x 0.100 x 0.100 mm^3	
Theta range for data collection	3.912 to 64.996°.	
Index ranges	-21<=h<=20, -15<=k<=16, -23<=l<=24	
Reflections collected	42462	
Independent reflections	8332 [R(int) = 0.1868]	
Completeness to theta = 64.996°	99.4 %	
Absorption correction	Semi-empirical from equivalents	
Max. and min. transmission	56 and 0.35	
Refinement method	Full-matrix least-squares on F^2	
Data / restraints / parameters	8332 / 661 / 666	

Goodness-of-fit on F^2	1.016
Final R indices [I>2sigma(I)]	R1 = 0.0858, wR2 = 0.2228
R indices (all data)	R1 = 0.1659, wR2 = 0.3100
Extinction coefficient	0.00031(5)
Largest diff. peak and hole	1.364 and -1.086 e.Å^{-3}

Table S2. Atomic coordinates (x 10^4) and equivalent isotropic displacement parameters (Å^{2}x 10^3) for $NaMo_{12}$. U(eq) is defined as one third of the trace of the orthogonalized U^{ij} tensor.

	x	y	z	U(eq)
C(1)	6931(9)	3952(18)	3529(10)	106(5)
C(2)	6335(11)	4051(19)	3813(10)	115(5)
C(3)	5590(10)	3720(20)	3448(11)	119(5)
C(4)	5440(10)	3365(19)	2799(11)	117(5)
C(5)	6026(12)	3340(20)	2493(10)	121(6)
C(6)	6767(10)	3650(20)	2857(11)	116(5)
C(7)	7238(11)	674(15)	4393(15)	119(6)
C(8)	7064(12)	-308(15)	4362(15)	133(6)
C(9)	6340(13)	-624(14)	3967(16)	138(6)
C(10)	5773(12)	33(16)	3643(16)	135(6)
C(11)	5943(13)	1011(15)	3670(16)	139(6)
C(12)	6666(13)	1329(13)	4076(16)	134(6)
C(13)	7241(12)	4575(18)	1403(16)	137(6)
C(14)	7094(13)	3603(17)	1229(17)	149(7)
C(15)	6355(15)	3309(15)	815(17)	153(7)
C(16)	5788(14)	4004(19)	546(17)	155(7)
C(17)	5915(13)	4968(18)	763(18)	153(7)
C(18)	6645(15)	5256(15)	1182(17)	149(7)
C(19)	5786(15)	6390(30)	4608(17)	178(8)
C(20)	5552(18)	6320(30)	3905(17)	184(8)
C(21)	4770(20)	6150(30)	3551(13)	189(8)
C(22)	4271(14)	5870(30)	3908(17)	184(8)

C(23)	4517(18)	5910(30)	4616(17)	189(8)
C(24)	5300(20)	6050(30)	4963(13)	189(8)
O(1)	8309(7)	3392(9)	4405(7)	76(3)
O(2)	8323(7)	4599(10)	3478(7)	76(3)
O(3)	7879(7)	5124(9)	4482(7)	78(4)
O(4)	9170(7)	6108(9)	4308(6)	70(3)
O(5)	9766(7)	3746(9)	4229(6)	73(3)
O(6)	9127(7)	4480(9)	5565(7)	75(3)
O(8)	8464(10)	5231(11)	6500(8)	101(5)
O(9)	9027(9)	2953(11)	6427(8)	97(4)
O(10)	9541(7)	2634(9)	5257(6)	74(3)
O(11)	8130(10)	1915(11)	5283(8)	100(5)
O(12)	8662(8)	225(10)	5251(9)	95(4)
O(13)	8588(8)	1338(10)	4303(7)	83(4)
O(15)	10017(9)	1733(9)	4178(7)	90(4)
O(16)	10047(8)	3273(10)	2994(7)	82(4)
O(17)	8594(8)	4032(10)	2272(7)	88(4)
O(18)	9584(8)	5225(10)	3276(7)	79(3)
O(19)	8624(10)	5275(14)	1386(8)	112(5)
O(20)	8131(9)	5735(11)	2339(7)	97(5)
O(21)	9043(9)	7198(9)	3109(8)	88(4)
O(23)	8488(9)	7906(10)	4385(8)	93(4)
O(24)	7195(8)	6958(11)	4499(9)	103(5)
O(25)	8627(7)	6392(9)	5393(6)	76(3)
O(26)	7133(9)	5757(11)	5426(9)	105(5)
O(27)	6840(30)	7490(30)	5610(20)	149(14)
O(27’)	6400(70)	7290(90)	5520(60)	160(20)
O(7)	7610(30)	3730(60)	5440(40)	82(12)
O(14)	8667(14)	2570(30)	3286(12)	78(6)
O(22)	7695(12)	6520(30)	3401(15)	77(6)
S(1)	7415(13)	3720(30)	5537(15)	83(5)
S(2)	8446(18)	2520(30)	3047(16)	84(7)
S(3)	7401(15)	6550(40)	3250(20)	82(7)
Mo(1)	8194(1)	5031(1)	5651(1)	79(1)
Mo(2)	8654(1)	3224(1)	5597(1)	78(1)
Mo(3)	9287(1)	2486(1)	4190(1)	76(1)

Mo(4)	9300(1)	3716(1)	3234(1)	76(1)
Mo(5)	8674(1)	6158(1)	3322(1)	79(1)
Mo(6)	8226(1)	6741(1)	4340(1)	80(1)
Na(1)	10000	5000	5000	78(3)
P(1)	8197(3)	1085(4)	4829(3)	84(2)
P(2)	8207(4)	4912(5)	1867(3)	92(2)
P(3)	6778(4)	6640(5)	5007(4)	107(2)
P(4)	7903(3)	4275(4)	4000(3)	76(1)
O(28)	8409(19)	7700(20)	6417(17)	106(10)
O(29)	8720(20)	8470(20)	2341(16)	105(10)
O(30)	8030(40)	9280(50)	2950(40)	250(30)
O(31)	10276(16)	5940(20)	2261(14)	140(10)
O(32)	7820(30)	1260(40)	2410(30)	93(16)
O(33)	9612(18)	-560(20)	4485(18)	101(9)
O(34)	9950(20)	-1040(30)	3410(20)	128(12)
O(35)	6210(30)	6360(40)	2330(20)	159(17)

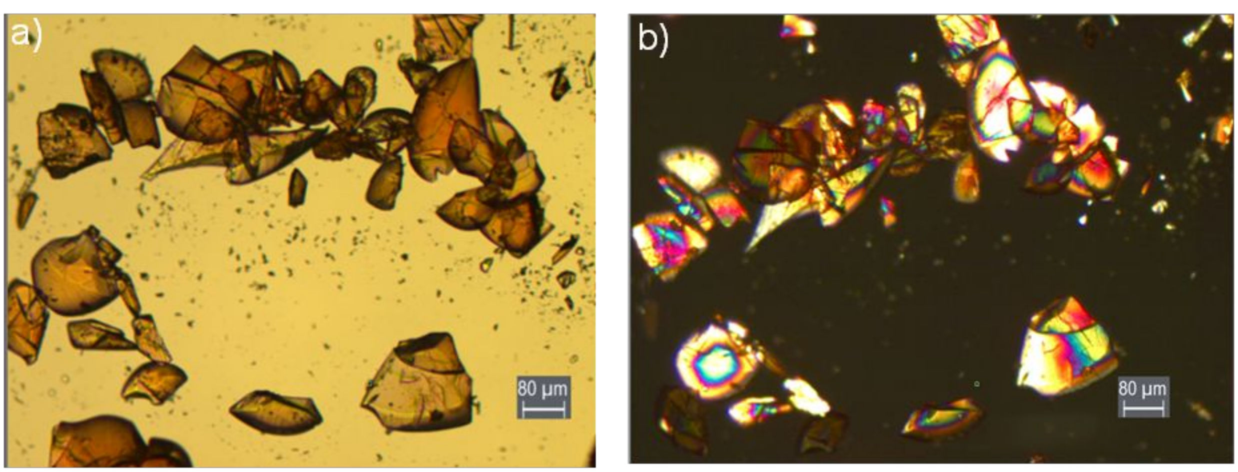

Figure S1. Optical microscopic images of crystals a) without and b) with polarizer.

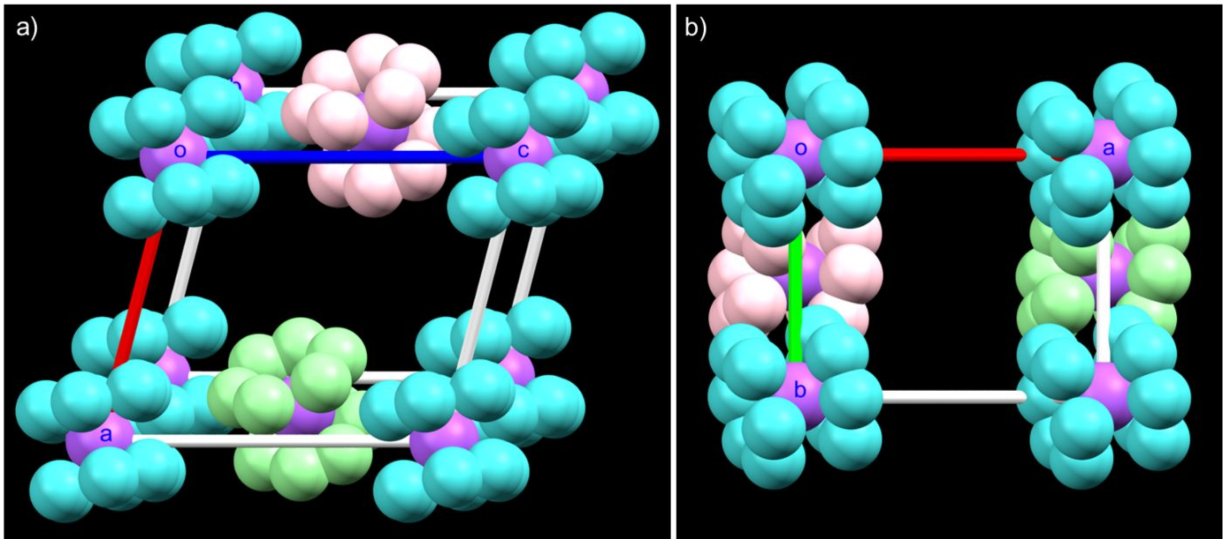

Figure S2. Unit cell packing of $NaMo_{12}$ unit of the cocrystal along a) b and b) c crystallographic axis. Color labels: sky blue = Mo for Mo_{12} cluster, light green = Mo for $Mo_{12}@S_2$ cluster, pink = Mo for $Mo_{12}@S_6$ cluster, purple = sodium.

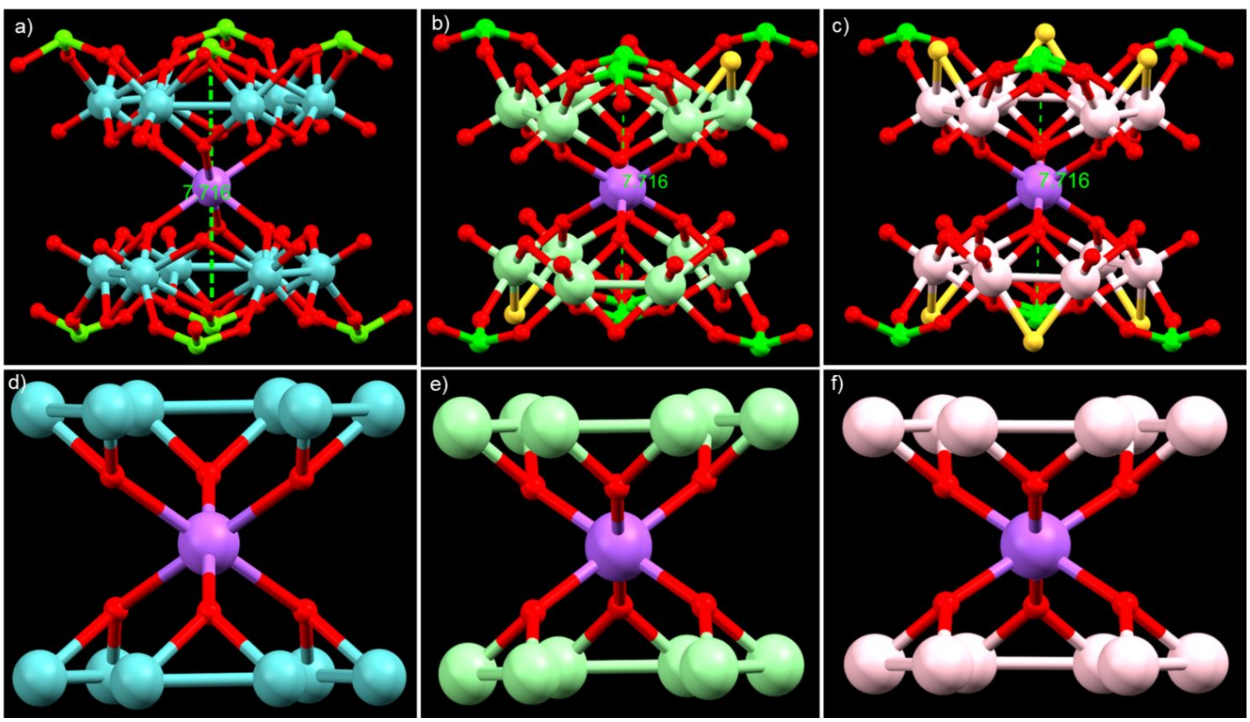

Figure S3. Structural model of the kernels of a) Mo_{12}, b) $Mo_{12}@S_2$, and c) $Mo_{12}@S_6$ clusters without PPA ligands. $NaMo_{12}O_6$ inner kernel framework of d) Mo_{12}, e) $Mo_{12}@S_2$ and f) $Mo_{12}@S_6$ clusters. Color code: sky blue, light green and pink = Mo; yellow = S; red = O, green = P, purple = Na.

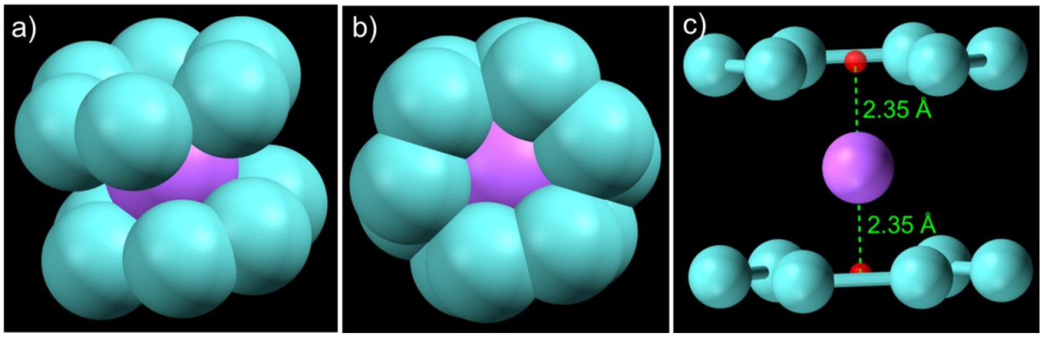

Figure S4. Space filling model of $NaMo_{12}$ unit for Mo_{12} cluster along a) side view and b) top view. C) The distance between sodium and the centrode of Mo_6 unit.

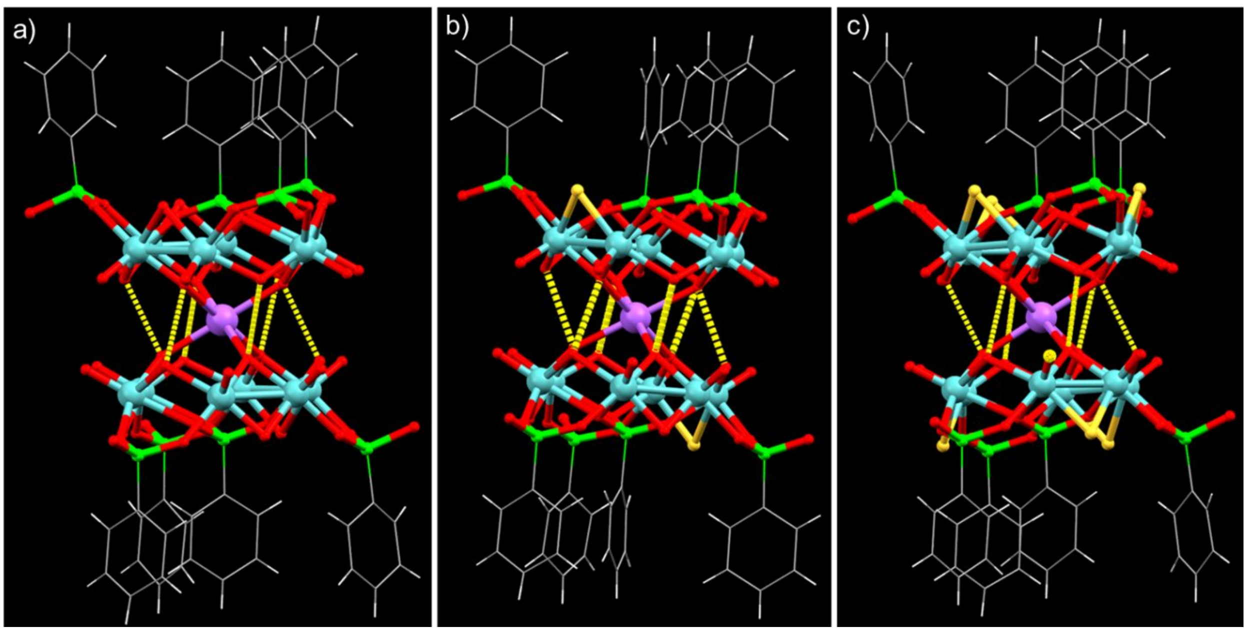

Figure S5. Short contact O···O interactions between two dumble-shaped units for a) Mo_{12}, b) $Mo_{12}@S_2$ and $Mo_{12}@S_6$ clusters.

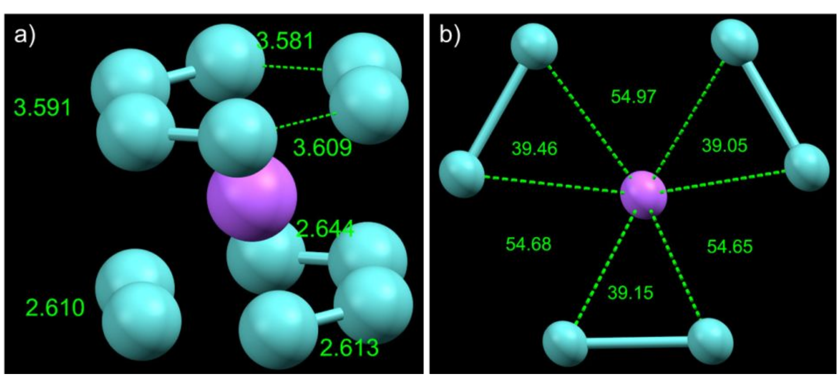

Figure S6. A) Mo-Mo bond distances of Mo_6 units, and b) the respective Mo-Na-Mo bond angles for Mo_{12} cluster.

Table S3. Comparative Mo-O/ Mo-S bond distances of $[Mo_6S_2O_{10}(C_6H_5PO_3)_4]$ unit.

Type of bonds	Mo-O distance (in Å)	Mo-S distance (in Å)
Mo-O (isolated O)	1.680, 1.690, 1.693, 1.695, 1.671, 1.699	
Mo-O (central P of PPA)	2.308, 2.364, 2.296, 2.333, 2.325, 2.360	
Mo-O /Mo-S (dangling O/S)	2.111, 2.118	2.119, 2.142, 2.125, 2.167
Mo-O (peripheral P of PPA)	2.049, 2.052, 2.088, 2.052, 2.091, 2.020	

Table S4. Comparative P-O bond distances of different PPA ligands bonded with the cluster.

PPA ligand	P-O bond distance (in Å)
Central PPA	1.533, 1548, 1.567
Peripheral PPA (Unit 1)	1.519, 1.537, 1.619 (free)
Peripheral PPA (Unit 2)	1.510, 1.512, 1.558 (free)
Peripheral PPA (Unit 3)	1.519, 1.532, 1.510 (free)

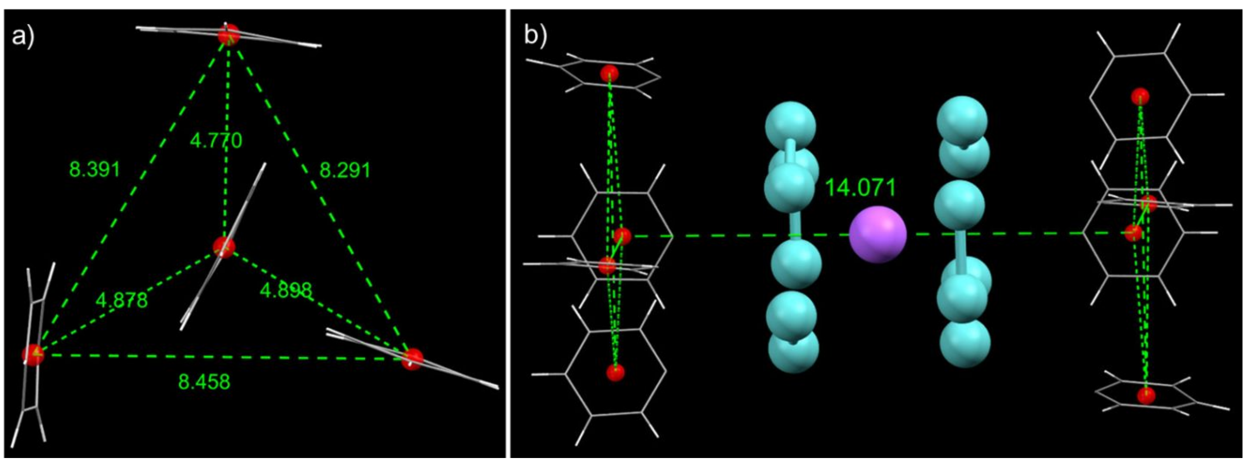

Figure S7. A) Interatomic distances of central P and peripheral P of PPA ligands. B) The distance between the centroids of two apexes of the cluster. These distances are similar for all three clusters.

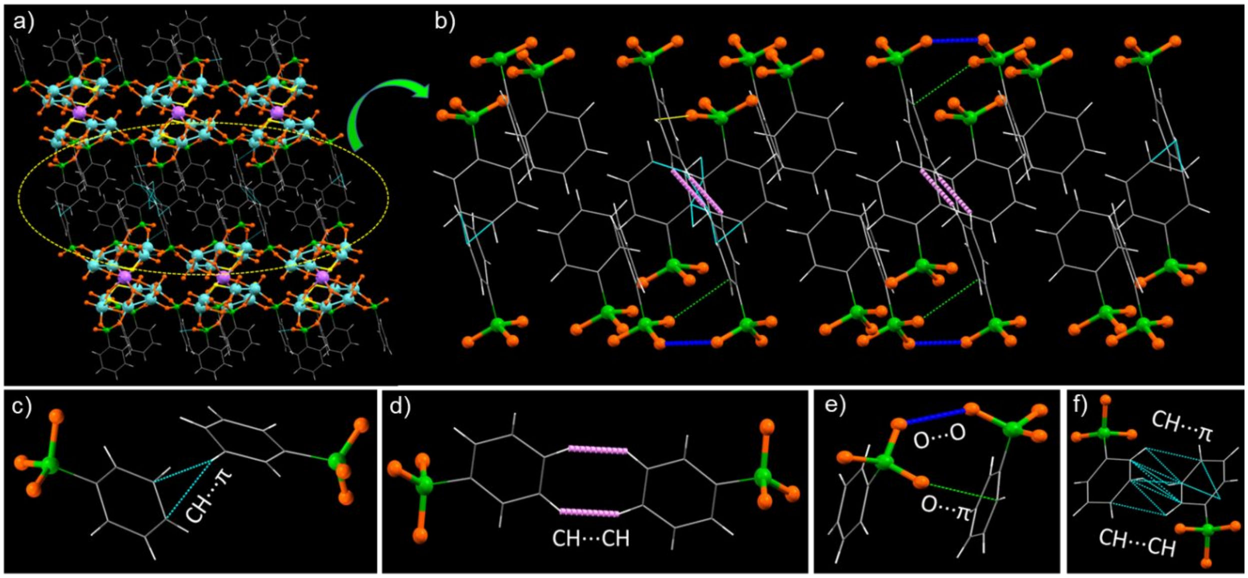

Figure S8. A) Intercluster packing shows different short contact interactions between peripheral benzene rings of the PPA ligands. B-f) Expanded view of these interactions with marked distances.

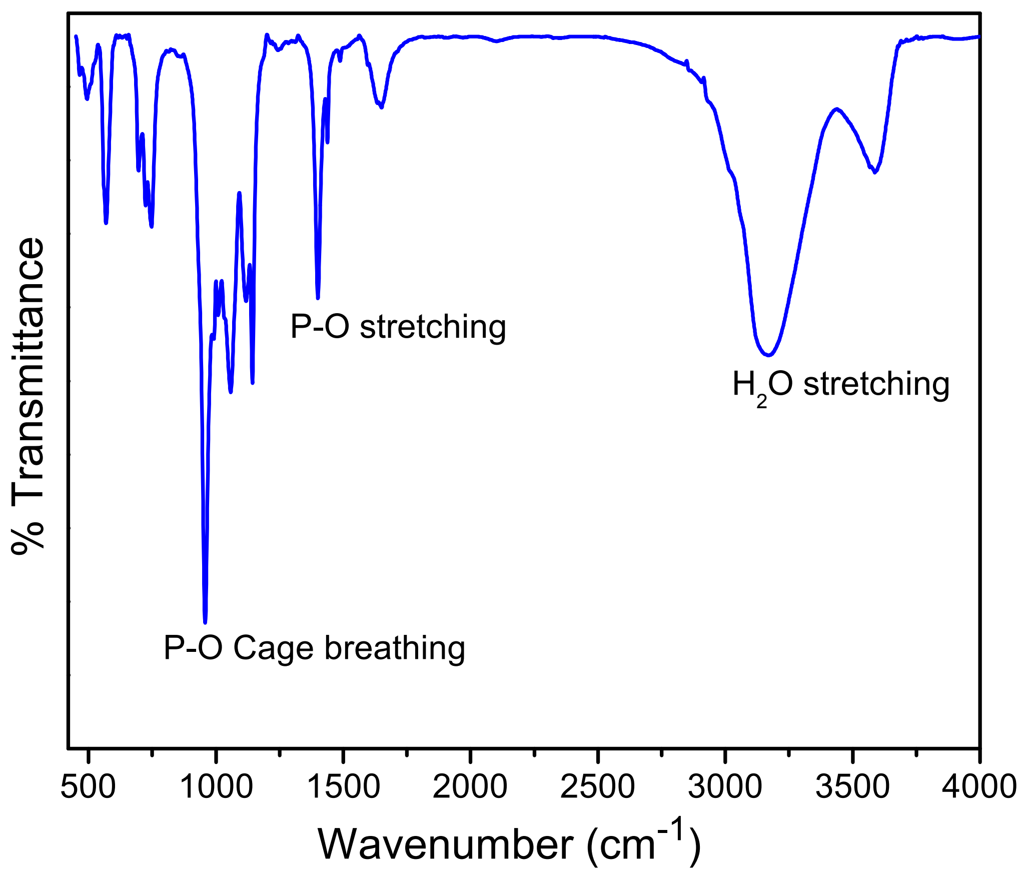

Figure S9. FT-IR spectrum of co-crystallized molybdenum oxo-sulfido clusters with respective peak assignments.

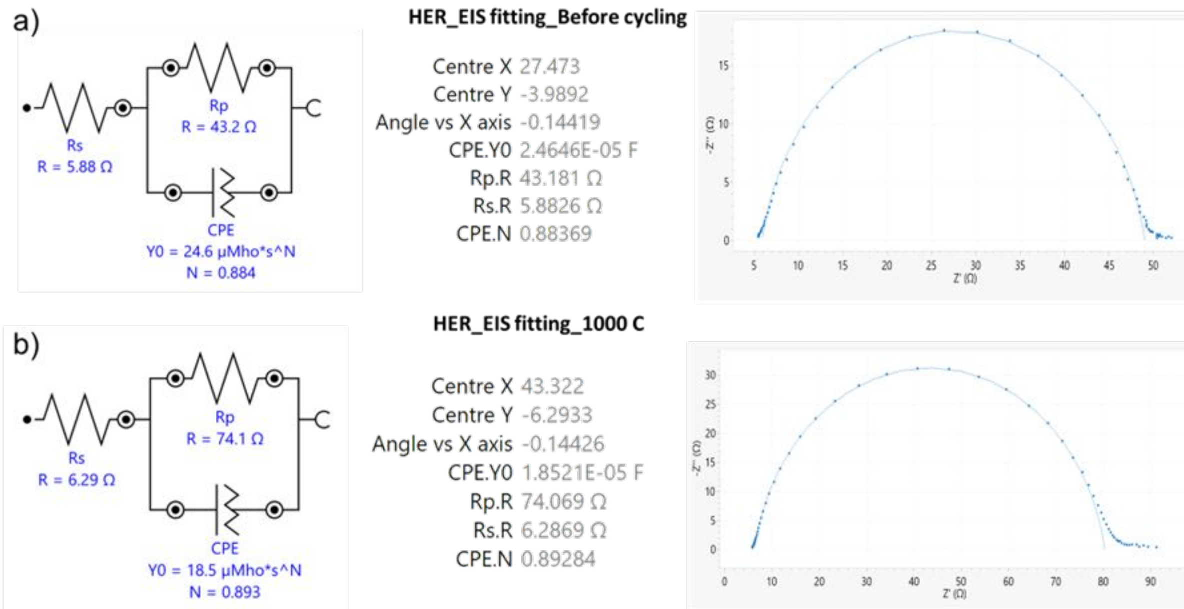

Figure S10. Randles circuit and Nyquist plot fitting of the EIS spectra for (a) HER on the pristine Mo_{12}-TC catalyst and (b) HER on the Mo_{12}-TC catalyst after 1000 cycles.

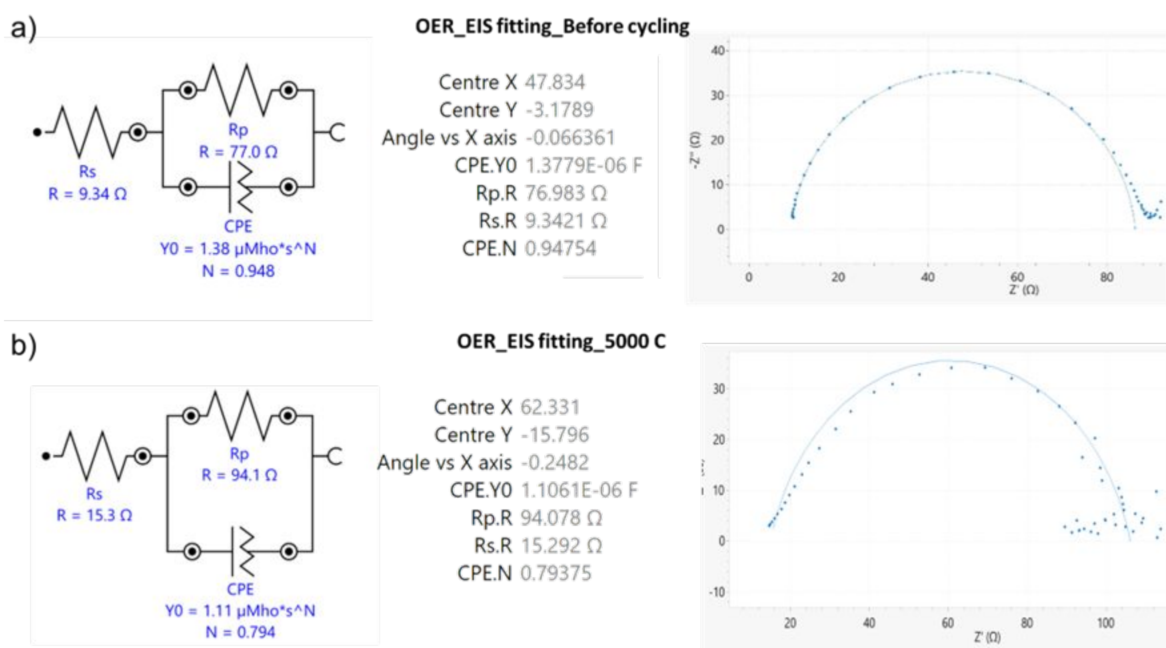

Figure S11. Randles circuit and Nyquist plot fitting of the EIS spectra for (a) OER on the pristine Mo_{12}-TC catalyst and (b) OER on the Mo_{12}-TC catalyst after 5000 cycles.

Table S5. EIS (Nyquist plot) fitting parameters for HER and OER on Mo_{12}-TC catalyst from the Randles equivalent circuits provided in Figure S10 and Figure S11. Rs stands for solution/series resistance, Rp denotes the charge transfer resistance or R_{CT} and CPE represents the constant phase element.

Condition	Rs (Ω)	Rp (Ω)	CPE.Y0 (F)	CPE.N
HER Before cycling	5.883	43.181	2.465e-5	0.884
HER After 250 cycles	6.206	50.332	2.417e-5	0.894
HER After 1000 cycles	6.287	74.069	1.852e-5	0.893
OER Before cycling	9.342	76.983	1.3783-6	0.948
OER After 1000 cycles	10.469	70.816	1.408e-6	0.925
OER After 2000 cycles	12.651	76.464	1.325e-6	0.884
OER After 5000 cycles	15.292	94.078	1.106e-6	0.794

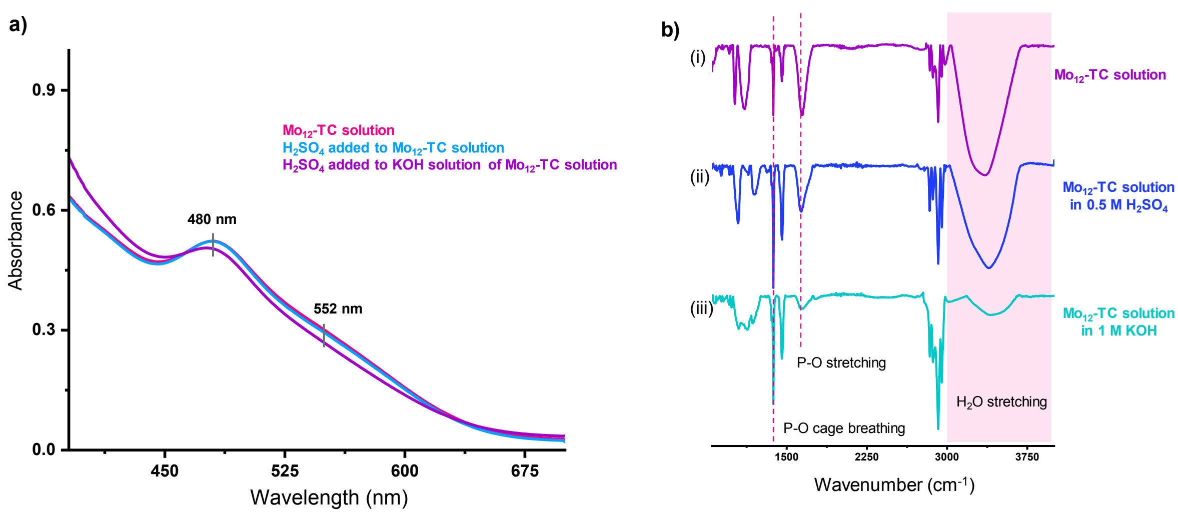

Figure S12. a) Comparative a) UV-vis absorption and b) FTIR spectra of Mo_{12}-TC, Mo_{12}-TC in 0.5 M H_2SO_4 (1:1 methanol: water), and Mo_{12}-TC in 1 M KOH (1:1 methanol: water) solutions. IR spectra were measured in Attenuated Total Reflectance Fourier Transform Infrared (ATR-FTIR) mode by placing the respective solutions on the ATR crystal.

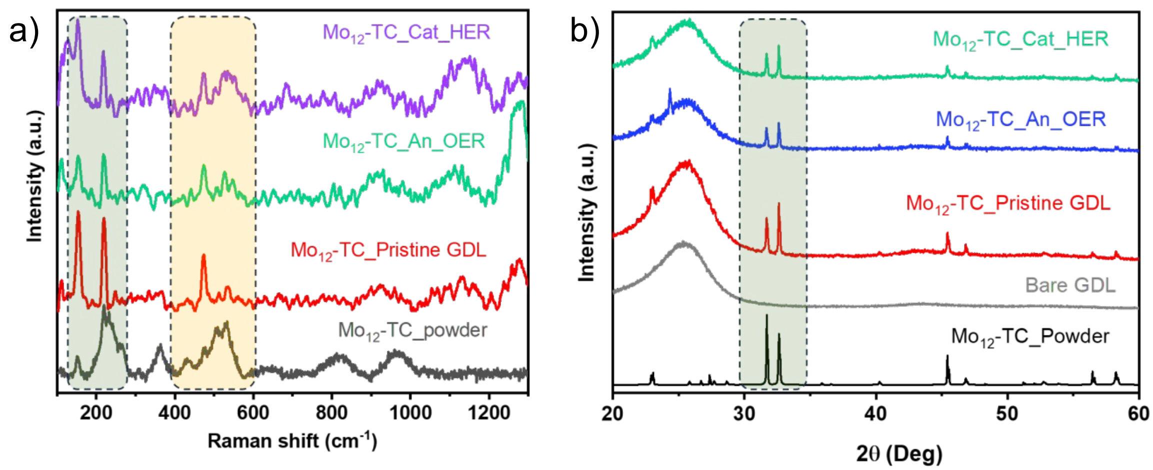

Figure S13. Comparative (a) Raman spectra and (b) XRD patterns of Mo_{12}-TC at different electrochemical conditions.

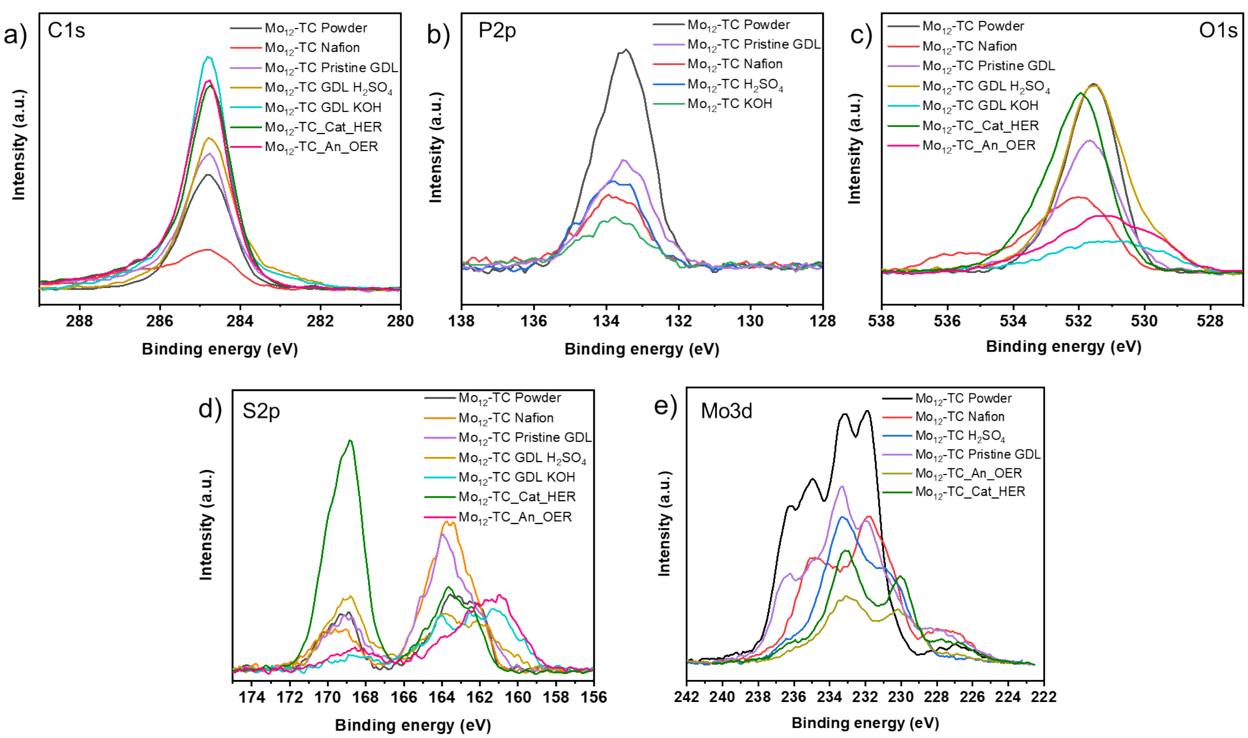

Figure S14. Comparative XPS elemental spectra of Mo_{12}-TC under different electrochemical conditions.

Table S6. Atomic % of the catalyst from XPS at different electrochemical conditions.

Sample	%C	%Mo	%O	%P	%S
Mo_{12} Pristine electrode	58.97	5.51	26.18	2.25	5.51
Mo_{12} HER	60.72	2.48	28.14	0.52	8.13
Mo_{12} electrode H_2SO_4	50.38	6.36	34.96	3.4	4.9
Mo_{12} OER	70.25	0.7	22.76	0.14	6.16
Mo_{12} electrode KOH	82.05	0.81	11.4	0.92	4.82
Mo_{12} Powder	45.5	8.43	36.23	4.39	5.46
Mo_{12} Nafion	60.43	5.23	24.1	1.97	8.27
Mo_{12} H_2SO_4	21.08	3.96	60	1.89	13.07
Mo_{12} KOH	70.7	1.82	21.95	1.13	4.4

Table S7. Atomic % of the catalyst from XPS at different electrochemical conditions

Sample	%Mo	%P	%S
Mo_{12} Pristine electrode	37.12	15.69	47.69
Mo_{12} HER	22.79	4.58	72.63
Mo_{12} electrode H_2SO_4	43.37	23.28	33.45
Mo_{12} OER	10.04	1.93	88.03
Mo_{12} electrode KOH	12.42	13.98	73.6
Mo_{12} Powder	46.12	24	29.87
Mo_{12} Nafion	33.81	12.73	53.45
Mo_{12} H_2SO_4	20.91	10	69.09
Mo_{12} KOH	24.7	15.41	59.89

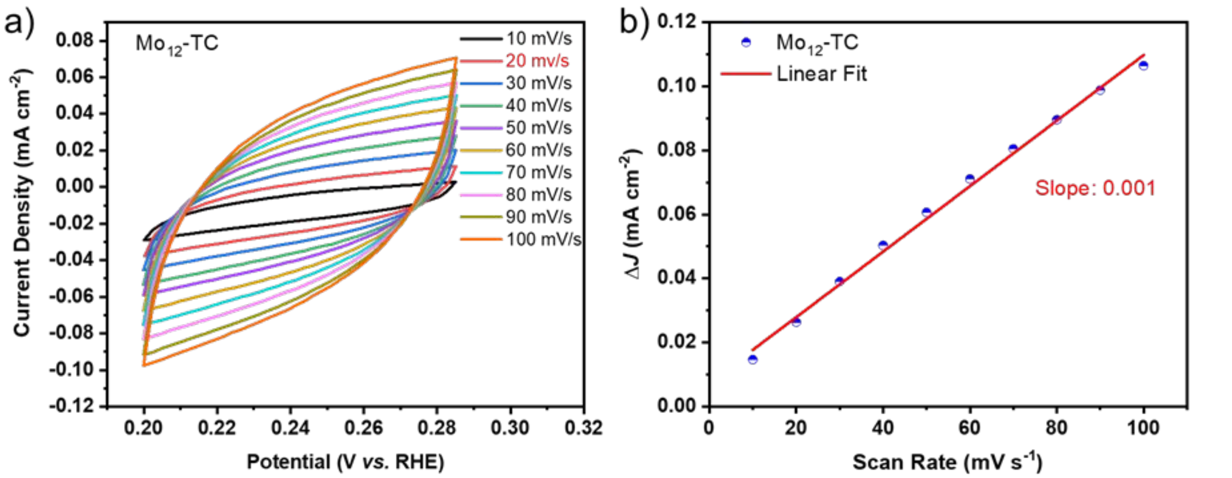

Figure S15. (a) CV at different scan rates in H_2SO_4 for the Mo_{12}-TC coated electrode and (b) ΔJ ($|j_{Cat}$-$j_{An}|$) vs. scan rate plot showing a slope of 0.001 corresponding to a C_{dl} of 0.5 $mFcm^{-2}$.

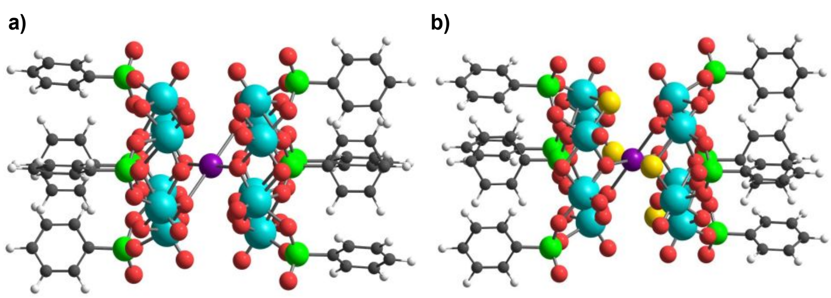

c)

Bond/Angle Type	Bond Length (Å)
Na-O	2.65
Mo-S	2.40
Mo-O (μ_2-Mo-O-Mo)	1.95
Mo-O (μ_3-Mo-O-P)	2.38
Mo-O (Terminal)	1.70
P-O	1.55

Figure S16. a) DFT optimized structure of a) Mo_{12} and b) $Mo_{12}@S_4$ cluster. c) Selected bond length and angles of the cluster. Atomic color code: sky blue = Mo; yellow = S; red = O, green = P, purple = Na, black = C, white = hydrogen.

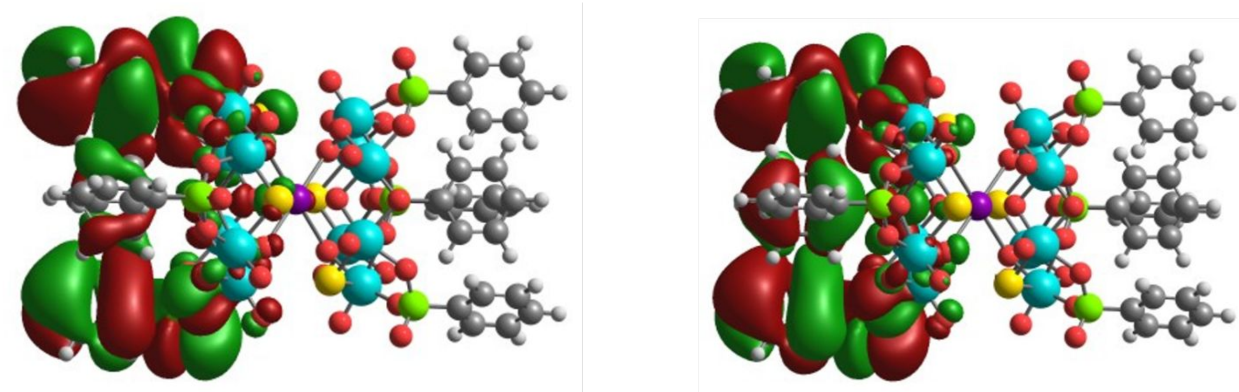

HOMO **LUMO**

E=-7.072 eV **E=-6.756 eV**

Figure S17. Electron density maps of the frontier molecular orbitals of the cluster. The energy of the respective orbitals are marked here. Green and dark red indicate positive and negative isosurfaces are plotted at 0.015 eV/Å^3. Atomic colors are the same with the earlier figures.

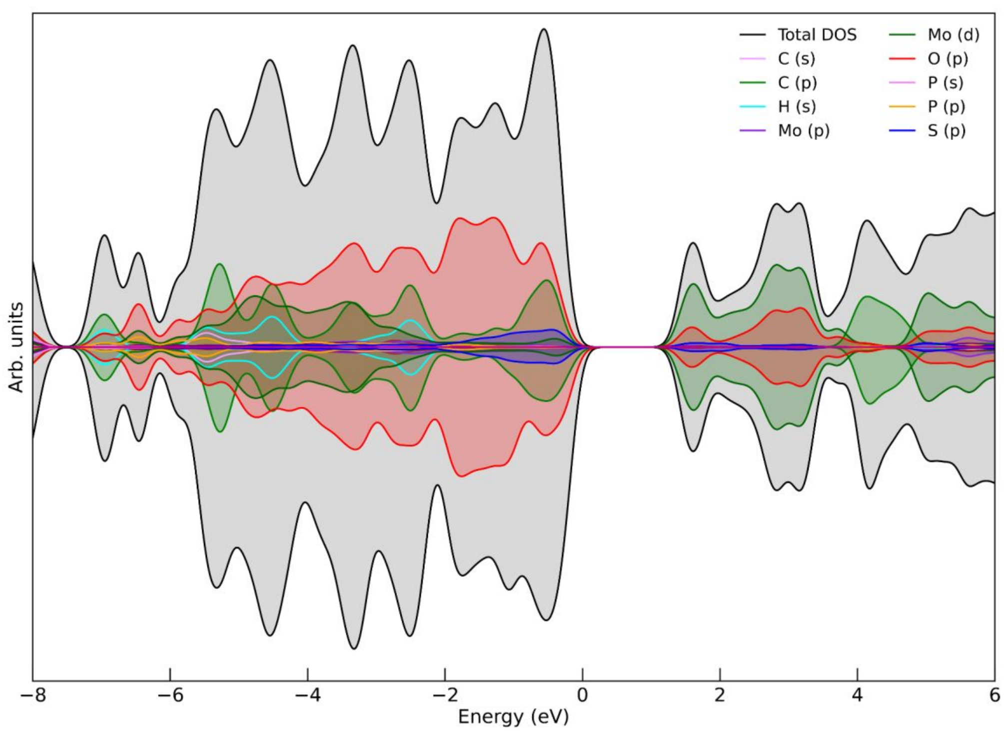

Figure S18. Total density of state (DOS) and projected density of states (PDOS) spectral profile of the respective elements of these clusters.

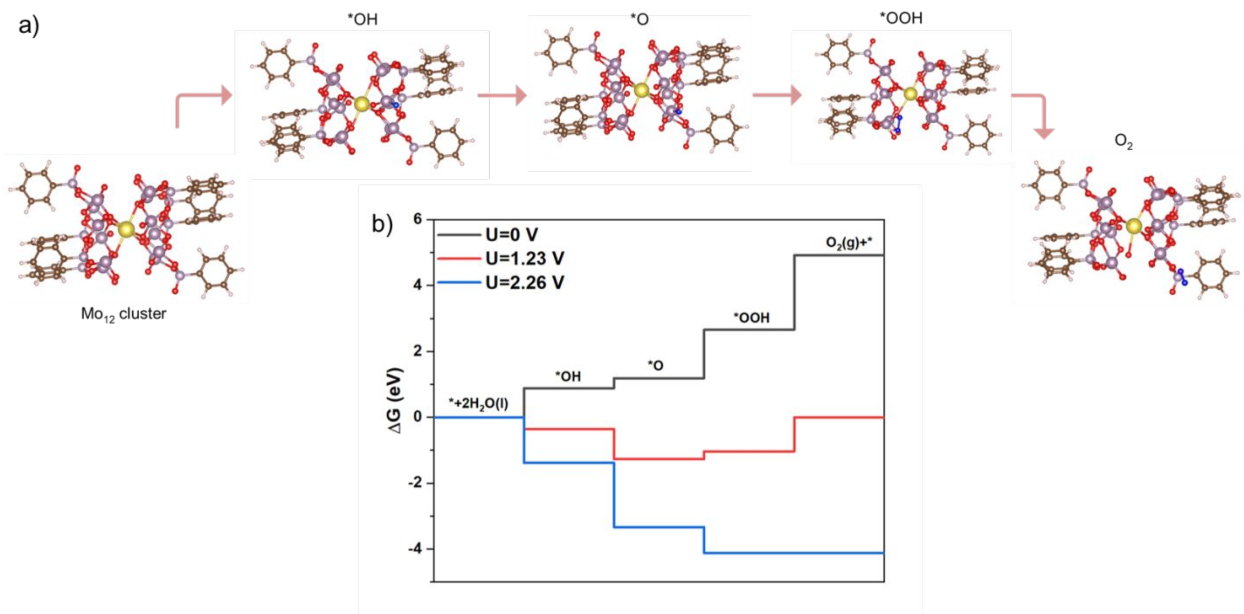

Figure S19. a) Structural representation of Mo_{12} cluster and its adsorption configurations of *OH, *O, and *OOH adduct intermediates and O_2 end product involved in OER. Atomic color code: Mo: purple, Na: Golden yellow, O: red, C: brown, H: pink, adsorbed O: blue. b) Calculated OER free energy profile for the Mo_{12} cluster at different potentials. The free energy profiles at 0 V (black), equilibrium potential of 1.23 V (red), and the limiting potential of 2.26 V (blue) are shown here.

References

(1) Perdew, J. P.; Burke, K.; Ernzerhof, M. Generalized Gradient Approximation Made Simple. *Phys. Rev. Lett.* **1996**, *77* (18), 3865–3868.

(2) Adamo, C.; Barone, V. Physically Motivated Density Functionals with Improved Performances: The Modified Perdew-Burke-Ernzerhof Model. *J. Chem. Phys.* **2002**, *116* (14), 5933–5940.

(3) Adamo, C.; Barone, V. Toward Reliable Density Functional Methods without Adjustable Parameters: The PBE0 Model. *J. Chem. Phys.* **1999**, *110*, 6158–6170.

(4) Mortensen, J. J.; Hansen, L. B.; Jacobsen, K. W. Real-Space Grid Implementation of the Projector Augmented Wave Method. *Phys. Rev. B - Condens. Matter Mater. Phys.* **2005**, *71* (035109), 1–11.

(5) Enkovaara, J.; Rostgaard, C.; Mortensen, J. J.; Chen, J.; Dułak, M.; Ferrighi, L.; Gavnholt, J.; Glinsvad, C.; Haikola, V.; Hansen, H. A.; Kristoffersen, H. H.; Kuisma, M.; Larsen, A. H.; Lehtovaara, L.; Ljungberg, M.; Lopez-Acevedo, O.; Moses, P. G.; Ojanen, J.; Olsen, T.; Petzold, V.; Romero, N. A.; Stausholm-Møller, J.; Strange, M.; Tritsaris, G. A.; Vanin, M.; Walter, M.; Hammer, B.; Häkkinen, H.; Madsen, G. K. H.; Nieminen, R. M.; Nørskov, J. K.; Puska, M.; Rantala, T. T.; Schiøtz, J.; Thygesen, K. S.; Jacobsen, K. W. Electronic Structure Calculations with GPAW: A Real-Space Implementation of the Projector

Augmented-Wave Method. *J. Phys. Condens. Matter* **2010**, *22* (253202), 1–24.